HHS Public Access

Author manuscript

Clin Cancer Res. Author manuscript; available in PMC 2019 February 15.

Published in final edited form as:

Clin Cancer Res. 2018 February 15; 24(4): 821–833. doi:10.1158/1078-0432.CCR-17-1628.

Development of a function-blocking antibody against fibulin-3 as targeted reagent for glioblastoma

Mohan S. Nandhu[1,5], **Prajna Behera**[1,5], **Vivek Bhaskaran**[1], **Sharon L. Longo**[4], **Lina M. Barrera-Arenas**[5], **Sadhak Sengupta**[2], **Diego J. Rodriguez-Gil**[3], **E. Antonio Chiocca**[1], and **Mariano S. Viapiano**[1,4,5]

[1]Department of Neurosurgery, Brigham and Women's Hospital and Harvard Medical School, Boston MA

[2]Brain Tumor Laboratory, Roger Williams Medical Center, Providence RI

[3]Department of Biomedical Sciences, East Tennessee State University, Johnson City TN

[4]Department of Neurosurgery, SUNY Upstate Medical University, Syracuse, NY

[5]Department of Neuroscience and Physiology, SUNY Upstate Medical University, Syracuse, NY

Abstract

Purpose—We sought a novel approach against glioblastomas (GBM) focused on targeting signaling molecules localized in the tumor extracellular matrix (ECM). We investigated fibulin-3, a glycoprotein that forms the ECM scaffold of GBMs and promotes tumor progression by driving Notch and NF-κB signaling.

Experimental Design—We used deletion constructs to identify a key signaling motif of fibulin-3. A monoclonal antibody (mAb428.2) was generated against this epitope and extensively validated for specific detection of human fibulin-3. mAb428.2 was tested in cultures to measure its inhibitory effect on fibulin-3 signaling. Nude mice carrying subcutaneous and intracranial GBM xenografts were treated with the maximum achievable dose of mAb428.2 to measure target engagement and anti-tumor efficacy.

Results—We identified a critical 23-amino acid sequence of fibulin-3 that activates its signaling mechanisms. mAb428.2 binds to that epitope with nanomolar affinity and blocks the ability of fibulin-3 to activate ADAM17, Notch, and NF-κB signaling in GBM cells. mAb428.2 treatment of subcutaneous GBM xenografts inhibited fibulin-3, increased tumor cell apoptosis, and enhanced the infiltration of inflammatory macrophages. The antibody reduced tumor growth and extended survival of mice carrying GBMs as well as other fibulin-3-expressing tumors. Locally-infused mAb428.2 showed efficacy against intracranial GBMs, increasing tumor apoptosis and reducing tumor invasion and vascularization, which are enhanced by fibulin-3.

Corresponding Author: Mariano S. Viapiano, PhD, Department of Neuroscience and Physiology, SUNY Upstate Medical University, 505 Irving Ave, IHP Building, Rm #4604, Syracuse, NY (13210), Tel: (315) 464-7738, viapianm@upstate.edu.

Conflict of Interest: MSN, EAC and MSV are co-inventors in the patent application "*anti-fibulin antibodies and uses thereof*" submitted to USPTO (#15/124,826; 2016). The authors do not have other conflicts of interest.

Conclusions—To our knowledge this is the first rationally-developed, function-blocking antibody against an ECM target in GBM. Our results offer a proof of principle for using "anti-ECM" strategies towards more efficient targeted therapies for malignant glioma.

Keywords

antibody therapy; brain cancer; extracellular matrix; fibulin; Notch pathway; NF-κB pathway; ADAM17; target engagement

Introduction

Glioblastomas (GBMs) are the most common malignant tumors originating in the CNS (1) and remain one of the deadliest form of cancer despite continuous advances for their treatment (2). Therapeutic strategies for GBMs are stymied by the heterogeneity of these tumors and their invasive behavior, which make them highly resistant to therapy and facilitate recurrence (3–5). There is a dire need for strategies capable of overcoming GBM dispersion and heterogeneity, in order to increase efficacy against tumor cells that may reside in different niches and express different molecular signatures.

The extracellular matrix (ECM) that fills the parenchyma of malignant gliomas has unique composition and structure compared to other solid tumors (6, 7). It contains remnants of the original neural ECM rich in hyaluronic acid and proteoglycans (8, 9) but also includes collagens and other fibrillar proteins produced *de novo* by tumor cells, resulting in a unique scaffold that supports GBM cell adhesion and dispersion (10). Prior work describing ECM molecules in malignant gliomas (6, 7, 11–13) and clonal and regional profiling of GBMs ((14, 15) and http://glioblastoma.alleninstitute.org), suggest that there may be considerable similarity of ECM components across GBM molecular subtypes and between tumor regions. Structural ECM molecules could therefore be useful molecular targets localized all over the tumor parenchyma, adjacent to GBM cells with different phenotypes and genotypes. Accordingly, ECM disruption could be a feasible approach to strike multiple populations of tumor cells surrounded by a common matrix scaffold. This idea has been successfully tested in experimental models, targeting for example GBM-enriched polysaccarides and proteoglycans to increase therapeutic delivery (16, 17) and to disrupt tumor growth and invasion (18, 19). An antibody against the ECM scaffolding protein tenascin-C has even advanced to the clinical stage and completed phases I and II clinical trials (20, 21). However, two major limitations for these strategies have been the difficulty to identify functional motifs underlying the pro-tumoral functions of ECM proteins, and the absence of reagents to disrupt signaling initiated or regulated by these ECM molecules.

Fibulin-3 is an ECM glycoprotein normally found in connective tissues, forming fibrils associated to elastin and collagen (22). This protein is sparsely detected in the body and is essentially absent in adult brain (23). However, fibulin-3 is highly expressed in GBMs (24), where it gains novel functions as autocrine/paracrine activator of Notch and NF-κB signaling, which have not been described in normal tissues (25–27). Fibulin-3 enhances GBM invasion, vascularization, and survival of the tumor-initiating population, correlating with poor patient survival and acting as a marker for regions of active tumor progression in

GBM (26, 28) and other invasive cancers (29–31). The low expression of fibulin-3 in normal tissues, high enrichment in GBMs, and non-structural functions in these tumors make it an appealing target to test “anti-ECM” strategies. Approaches focused on blocking the novel functions of fibulin-3 in GBM should have limited off-target effects because this protein is not expressed in normal brain or known to act as a soluble signaling factor in other tissues.

We report here the development and pre-clinical characterization of a novel antibody that blocks a unique functional motif in fibulin-3, resulting in complete inhibition of its signaling functions in GBM cells. This antibody has anti-tumor efficacy against GBMs and other fibulin-3-secreting solid tumors, being the first example of a rationally-developed, function-blocking antibody against an ECM protein and capable of inhibiting cancer signaling. We propose this antibody as a proof-of-concept of ECM-targeting approaches to potentiate current therapies against GBM.

Materials and Methods

DNA and protein reagents

A full-length clone of human fibulin-3 (1,479 bp) was cloned in pcDNA3.1(+) as described (24). Deletion constructs lacking N-terminal sequences were generated by PCR. Reporter plasmids carrying firefly luciferase under control of Notch-dependent (pGL2Pro-CBF1-Luc) or NF-κB-dependent (pGL4.32/luc2P/NF-RE) promoters have been described elsewhere (25, 26). Purified fibulin-3 was from R&D Systems (Minneapolis, MN). Purified, endotoxin-free, non-immune mouse IgG was from Molecular Innovations (Novi, MI). Fibulin-3 peptides, both free and conjugated to bovine serum albumin (BSA) or Keyhole limpet hemocyanin (KLH) were synthesized and purified at Yenzym Antibodies (San Francisco, CA). Amino acids in the peptides were numbered to follow their corresponding position in full-length human fibulin-3. Antibodies and primer sequences used in this work are listed in Suppl. Tables I and II.

Cells and tissue specimens

GBM cell lines, GBM stem-like cells (GSCs), and HEK293 cells were cultured following described standard methods (24, 25, 28). Renal cell carcinoma SN12C and colon adenocarcinoma COLO201 cells were cultured in high-glucose DMEM with 10% fetal bovine serum and standard antibiotics, while mesothelioma H226 cells were cultured in RPMI-1640 medium with the same supplements. Endogenous fibulin-3 was detected by qRT-PCR and Western blot (24) in all cells except COLO201 and HEK293. Cells were authenticated and confirmed free of contaminants at the IDEXX-Research Animal Diagnostic Laboratory (Columbia MO). Frozen specimens of GBM and pathologically normal brain were procured from NCI’s Cooperative Human Tissue Network and SUNY Upstate University Hospital, with patient consent and institutional review board approval. Paraffin-embedded tissue sections were from US Biomax (Rockville, MD).

Antibody production and validation

The sequence N-T^{25}YTQCTDGYEWDPVRQQCK^{43}DIDE^{47}-C (“DSL-like” sequence) from human fibulin-3 was chosen as immunogen to produce monoclonal antibodies. To

retain the internal disulfide bridge Cys^{29}-Cys^{42} (23), the peptide was not conjugated with maleimide to KLH; instead, an N-terminal lysine was added for conjugation using N-hydroxysuccinimide ester and the internal Lys^{43} was changed to arginine (see Figure 1E). Mouse monoclonal antibodies were produced at the Dana Farber Cancer Institute Monoclonal Antibody Core Service (Boston MA). Hybridoma clones were chosen through multiple rounds of subcloning as indicated in Suppl. Figure S1. The final anti-fibulin-3 clone (mAb428.2.3C11.H11.G3) was nicknamed *mAb428.2.*

Binding of mAb428.2 to fibulin-3 and BSA-conjugated DSL-like peptide was validated using indirect-ELISA. Briefly, microtiter plates were coated with fibulin-3 (200 ng/ml) or DSL-like peptide (1000 ng/ml), blocked with bovine albumin, and probed with mAb428.2 and anti-mouse secondary antibodies. Antibody binding was quantified by a colorimetric reaction using standard ELISA procedures. The antibody was also tested by Western blot (Figure 2) and dot blot (not shown) to confirm binding to purified fibulin-3. mAb428.2 was purified in low-endotoxin conditions (< 1 EU/mg) and equilibrated in phosphate-buffered saline, pH 6.5. The affinity of mAb428.2 for purified fibulin-3 was measured by surface plasmon resonance (Biacore 3000 biosensor) at room temperature. Standard biophysical analysis of mAb428.2 was performed at Wolfe Laboratories (Waltham, MA) and included size exclusion chromatography to determine polydispersity, isoelectrofocusing to determine pI, and differential scanning calorimetry to determine aggregation/solubility.

In vitro assays and histology

Cells and tissues were lysed and processed for Western blotting or semiquantitative real time PCR (qRT-PCR) using standard protocols (24, 25). Reporter cells carrying stably transfected Notch- or NF-κB-reporter plasmids were transfected with a *Renilla* luciferase plasmid (pGL4.75-Rluc/CMV, Promega) as loading control. Cells were stimulated with purified fibulin-3 (300 ng/ml) for 6h or transfected with fibulin-3 cDNA and used 24h after transfection. For a positive control of Notch activation, cells were transfected with the plasmid pSG5-FLAG-NICD carrying the constitutively-active Notch1 Intracellular Domain (*NICD*) (25). For a control of NF-κB activation, cells were treated with Tumor Necrosis Factor-alpha (TNFα; 10 ng/ml, 6h) as described (26). To measure ADAM17 proteolytic activity, cells were transfected with fibulin-3 constructs, lysed after 24h, and incubated with a fluorogenic ADAM17 substrate peptide (R&D Systems) as previously described (28). All transfections were performed in cultures adjusted to a density of $1x10^6$ cells/ml.

To measure cell invasion, GSC tumorspheres were labeled with a fluorescent dye (PKH26, Sigma-Aldrich), seeded on freshly prepared brain slices, and cultured for up to five days following our established protocols (24). The dispersion of the cells into brain tissue was imaged daily by fluorescence microscopy (24). A *Migration Index* was calculated as the ratio of area covered by the dispersed cells to the original area of the spheroids. Antibodies (200 μg/ml) were added to the organotypic cultures every 48h together with fresh culture medium.

Fibulin-3; 5-bromo-2′-deoxyuridine (BrdU); co-expressed macrophage markers (Iba1; Arginase-1); and the DNA-damage marker phospho-histone H2A.X were detected in tissue sections following previously described immunohistochemical protocols (28, 32, 33). Blood

vessels were stained with an antibody against mouse CD31; vessel length and density per tumor area were calculated using particle image analysis as described (28).

In vivo procedures

All animal experiments were performed in athymic mice (FoxN1$^{nu/nu}$, Envigo) following institutional approval at the Brigham and Women's Hospital and SUNY Upstate Medical University. mAb428.2 was prepared in lactated Ringers solution (pH 6.5) and confirmed free of endotoxins, mycoplasma, and rodent pathogens (Yale University Section for Comparative Medicine; New Haven, CT). Preliminary toxicity assays were performed in C57Bl/6 mice and Lewis rats, injected intravenously (IV) with mAb428.2 for eight consecutive days and monitored for up to 7 days after the final injection.

For sub-cutaneous (SC) tumor implantation, animals (N=8/group) received bilateral injections of 1x10^6 tumor cells (in 100 μL) without Matrigel™ adjuvant. Tumors were measured every other day with calipers and volumes were calculated as (length x width^2)/2. The larger of the two tumors per animal was used to decide treatment initiation and endpoint. When tumors reached a threshold of 100 mm^3 mAb428.2 was injected directly in the tumor mass (3 x 30 mg/kg q48h) or IV (8 x 30 mg/kg q24h). Animals were euthanized at a fixed endpoint 3 days after the last antibody injection, or monitored for overall survival and terminated when tumor volumes reached 1,000 mm^3. For intracranial tumor implantation, animals (N=8/group) were injected with 10,000 GBM stem-like cells in the right striatum (2 μL) and one week later intracranial cannulas were implanted to deliver mAb428.2 from a SC osmotic pump (Alzet #2001; 1.5 mg/mL antibody released at 1.0 μL/h for 8 days). Pumps were removed after the antibody was fully delivered and the animals were monitored for overall survival. All euthanized mice were perfused with phosphate-buffered saline and tissues were recovered for biochemical or immunohistochemical analyses. Subclass-specific secondary antibodies were used to detect intratumoral retention of mAb428.2 by Western blot of immunohistochemistry.

To detect antibody distribution in naïve and tumor-carrying mice, mAb428.2 was fluorescently labeled with DyLight-755 following the manufacturer's protocol (ThermoFisher antibody labeling kit #84538), injected IV at 5 mg/kg, and visualized using an in-vivo imaging system (Spectral Instruments Ami-X, Tucson AZ; Ex/Em=745/790 nm).

Statistics

In vitro experiments were repeated at least twice with 3–5 independent replicates each time; all results were represented as mean ± S.D. Animal studies were performed with N=5/group for fixed-endpoint and N=8/group for overall survival studies (to detect differences at least 50% larger than the S.D. of the groups, at power 80% and $p<0.05$). Bilateral tumors were averaged to calculate a mean tumor volume per animal. Blinding and randomization for animal studies followed the ARRIVE guidelines for animal research (34).

Results

An exposed N-terminal motif of fibulin-3 is critical for its signaling

Fibulin-3 increases canonical Notch (25, 27) and NF-κB (26, 35) signaling in tumor cells. The mechanism is not fully elucidated but includes activation of the cell-surface metalloprotease ADAM17, which cleaves (and activates) Notch receptors (28) and can also release TNFα to initiate NF-κB signaling (26). We therefore sought to identify a functional motif(s) of fibulin-3 critical for these signaling mechanisms.

Fibulin-3 has a unique N-terminal, EGF-like domain (Met^{1}-Ser^{106}) that includes a sequence (Thr^{25}-Cys^{70}) named "DSL-like" for its high homology to the canonical *Delta-Serrate-Lag* (DSL) motif present in Notch ligands (25). We have shown that this N-terminal domain is necessary and sufficient to activate Notch signaling (25), suggesting that disrupting this domain could affect molecular pathways regulated by fibulin-3.

To test this hypothesis we analyzed short sequences within the DSL-like motif and found that fibulin-3 lacking the sequence Thr^{25}-Glu^{47} ("fibulin-3ΔDSL", Figure 1A) was unable to activate Notch- and NF-κB reporters in U251MG GBM cells (Figure 1B–1D). The deletion did not affect fibulin-3 secretion (Figure 1C) or the activation of the reporters by their respective canonical signals (Figure 1B; 1D), suggesting a specific loss of fibulin-3 signaling function. In agreement, transfection of fibulin-3ΔDSL in U251MG cells failed to increase the expression of the Notch-dependent genes *HES5* and *MMP2* (Figure 1E), which are regulated by fibulin-3 in GBM (25, 26). Moreover, fibulin-3ΔDSL lacked any enhancing effect on ADAM17 catalytic activity (Figure 1F). In sum, deletion of the Thr^{25}-Glu^{47} sequence was sufficient to completely abolish the signaling functionality of fibulin-3.

Analysis of the sequence Thr^{25}-Glu^{47} of human fibulin-3 using the PHYRE2 Protein Fold Recognition Server (www.sbg.bio.ic.ac.uk/~phyre2 (36)) suggested that it is highly exposed on the globular head of the protein (22) and is well conserved among species (Figure 1G). We then set out to generate an antibody capable of binding and blocking this exposed functional motif. Because the sequence Thr^{25}-Glu^{47} contains two cysteines that may form an intramolecular bridge (23) we modified one amino acid in the sequence ($Lys^{43} \rightarrow$ Arg) to retain this feature in the peptide used for immunization (Figure 1E).

Characterization of mAb428.2, a novel anti-fibulin-3 antibody

The antibody mAb428.2 was confirmed to be a mouse IgG1 kappa. It has average pI=7.48, which limited its solubility in phosphate-buffered saline to approximately 5–6 mg/ml before noticeable aggregation. At concentration of 1 mg/ml in this buffer, mAb428.2 remained as >99% monomeric at room temperature.

mAb428.2 detected denatured fibulin-3 in reducing and non-reducing conditions (Figure 2A), suggesting that the presence of the disulfide bond in the epitope was not critical for recognition. The antibody did not cross-react with fibulin-4 and -5 (Figure 2B), or with fibulin-3ΔDSL lacking the target epitope (Figure 2C). Binding of mAb428.2 to BSA-conjugated DSL-like peptide or to purified fibulin-3 was competitively inhibited by free DSL-like peptide (Figure 2D–2E and Suppl. Figure S2A), suggesting that this epitope is the

only part of fibulin-3 recognized by the antibody. Binding of mAb428.2 to fibulin-3 was inhibited by the endogenous DSL-like sequence from human fibulin-3 (with Lys^{43}) and by the modified sequence used for immunization (with $Lys^{43}\rightarrow Arg$) (Figure 2F). Interestingly, a DSL-like peptide derived from mouse fibulin-3, which contains Ile^{38} instead of Val^{38}, was unable to displace the binding of mAb428.2, suggesting that our antibody may show poor to negligible recognition of mouse fibulin-3 (Figure 2F). Measurement of binding kinetics of mAb428.2 to purified human fibulin-3 revealed a high affinity binding with Kd= 5 ± 1 nM (Suppl. Figure S2B).

mAb428.2 also recognized native fibulin-3 in GBM tissues in a manner comparable to the antibody mAb3-5, which is a well-characterized antibody raised against human fibulin-3 for histology (37). mAb428.2 detected pericellular and diffusely localized fibulin-3 in low-grade astrocytoma and GBM, matching the staining of mAb3-5 that increases with tumor grade (25) (Figure 2G). None of these antibodies showed specific staining of normal adult brain. In frozen (non-paraffinized) tissues, both mAb3-5 and mAb428.2 detected a characteristic perivascular fibrillar pattern of fibulin-3 that we have observed restricted to human GBM blood vessels (Figure 2H and (28)). Further staining of live, dissociated GBM cells and fixed GBM tumorspheres (Suppl. Figure S3) confirmed that mAb428.2 detects fibulin-3 that accumulates in the intercellular ECM as well as peripherally associated to the membrane of the tumor cells.

Taken together, our results validate mAb428.2 as a novel antibody that recognizes human fibulin-3 with high affinity and specificity, under a variety of conditions and specimen preparations.

mAb428.2 is a function-blocking anti-fibulin-3 antibody

We first tested mAb428.2 on U251MG cells overexpressing fibulin-3. Transfected fibulin-3 cDNA increased the activity of a Notch-dependent reporter in these tumor cells; however, this effect was completely abolished by mAb428.2 in a time- and concentration-dependent manner (Figure 3A–3B). mAb428.2 also inhibited the enhancing effect of fibulin-3 on a NF-κB-dependent reporter (Figure 3C) and ADAM17 activity (Figure 3D). The antibody did not affect the direct activation of the Notch reporter by NICD or the NF-κB reporter by TNFα (Figure 3E), indicating that its effects were specific against fibulin-3. A pre-immune control IgG had no effects in any of these assays.

As additional confirmation we tested the effect of mAb428.2 against endogenous fibulin-3 secreted by GBM cells. mAb428.2 added to cell cultures for 24h reduced the expression of several Notch and NF-κB-regulated genes in U251MG cells as well as in mesenchymal-type GSCs that have high endogenous expression of fibulin-3 (25) (Figure 3F). Taken together, our results indicate that mAb428.2 is a function-blocking antibody against fibulin-3.

mAb428.2 inhibits fibulin-3 signaling in vivo, reduces tumor growth, and induces anti-tumor inflammation

For *in vivo* experiments mAb428.2 was injected IV once a day for eight days (to match the time needed to empty the reservoir of an osmotic pump for local delivery). We did not observe toxic effects in naïve mice treated with mAb428.2 up to 30 mg/kg or in Lewis rats

treated with an adjusted dose of 20 mg/kg (38). The animals did not show changes in weight or any signs of acute damage in normal tissues that contain fibulin-3, such as kidneys' glomeruli, connective tissue in articular joints, or retinal epithelium (Suppl. Figure S4).

To assess anti-tumor efficacy, mAb428.2 was tested against the highly aggressive GSC GBM34 (25). Tumor cells were implanted SC and treated with mAb428.2 or non-immune control IgG once the tumors reached a threshold volume of 100 mm^3. A preliminary test with direct intratumoral injections of mAb428.2 (3 x 30 mg/kg q48h) showed significant reduction of tumor volume and final weight measured at a fixed endpoint (Suppl. Figure S5A–S5B). Similar reduction in tumor growth was observed when the antibody was delivered IV (8 x 30 mg/kg q24h) suggesting that peripherally-delivered mAb428.2 reaches its target in the tumor mass (Figure 4A). Tumor tissues were subsequently processed to detect indicators of Notch and NF-κB signaling, including expression of Notch1 Intracellular Domain (active form of Notch1); Notch-regulated transcription factor Hes5; and phosphorylation of the NF-κB transcription factor RelA/p65. We observed significant downregulation of all these proteins in tumors treated with mAb428.2, both by direct intratumoral injection (Suppl. Figure S5C) and IV delivery (Figure 4B–4C).

Further analysis of the GBM34 tumors treated with mAb428.2 revealed increased expression of cleaved caspase-3 in the tumor mass (Figures 4D, 4F) and significant reduction of BrdU uptake (Figures 4E, 4G), suggesting a cytostatic and possibly cytotoxic effect of mAb428.2 treatment. Indeed, post-mortem examination revealed considerable necrosis in the core of mAb428.2-treated tumors (Suppl. Figure S5D).

The observation of widespread tumor apoptosis and necrosis *in vivo* (see also Figure 6C and comments in Suppl. Figure S6) was somewhat surprising because highly purified mAb428.2 did not reduce GBM cell viability significantly when added to cultures for 24–72h (not shown). Therefore, we explored if the antibody had caused any effects on immune cells that could help explain tumor cell death. Indeed, mAb428.2-treated tumors showed increased infiltration of macrophages (Iba1-positive cells; Figure 4H) and lower or absent expression of the M2-phenotype marker Arginase-1 in those macrophages (Figure 4I), compared to the control IgG treatment. In agreement with these histological findings, tumors treated with mAb428.2 and processed to measure mouse-specific mRNAs showed increased expression of inflammatory cytokines (IL-1β, IL-10 and gamma-interferon) and reduced expression of macrophage markers associated with the M2 phenotype (39) such as Arginase-1 (ARG1), CD163, and CD206 (Figure 4J). Moreover, mAb428.2 increased the mRNA expression of human-specific pro-inflammatory cytokines, derived from the tumor cells (Figure 4K). Taken together, the results suggested that mAb428.2 induces a marked anti-tumor reaction driven, in part, by inflammation and activation of innate immunity.

mAb428.2 extends survival of mice carrying fibulin-3-expressing tumors and disrupts GBM invasion and vascularization

We next evaluated the efficacy of mAb428.2 to extend survival of mice carrying fibulin-3-expressing SC tumors, including our two GSC-derived GBM models as well as cell lines (H226 and SN12C) chosen from the NCI-60 collection for their high expression of fibulin-3 (40) (Figure 5A). One additional cell line (COLO201) was chosen as negative control for its

negligible endogenous expression of fibulin-3. IV-injected mAb428.2 reduced tumor volume (Suppl. Figure S6) and significantly improved survival in all the fibulin-3-expressing models (Figure 5B–F), extending median survival by 28% (GBM09) to 64% (GBM34) in the GBM xenografts. However, mAb428.2 did not prolong the survival of mice carrying fibulin-3-negative COLO201 tumor cells (Figure 5D).

We also tested mAb428.2 against both GSC models implanted intracranially, but were unable to detect a survival improvement when the antibody was delivered peripherally (Figures 6A and S7A). However, when a comparable dose of antibody was infused into the intracranial tumor mass using an osmotic pump we observed again a significant increase in median survival (32%, Figure 6A), suggesting that mAb428.2 has anti-tumor efficacy when it is able to accumulate in the tumor parenchyma. Accordingly, a small biodistribution study using IV-injected, fluorescently-labeled mAb428.2 suggested that the antibody may be rapidly cleared from circulation but nevertheless accumulates in SC tumors and remains at peak level in the tumor for at least 24h after injection. In contrast, mAb428.2 fails to accumulate in intracranial tumors unless it has been locally delivered (Suppl. Figure S8A–S8D).

Further analysis of mAb428.2-treated intracranial tumors focused on tumor invasion, apoptotic resistance, and vascularization, all of which are enhanced by fibulin-3 (25, 28). We were unable to assess the effect of mAb428.2 on intracranial tumor dispersion *in vivo* due to the modest invasive profile and the large size of GBM09 and GBM34 tumors by the time that the animals could be euthanized. However, mAb428.2 caused significant inhibition of GSC invasion in cultured brain slices (Figure 6B), which is an accurate surrogate of *in vivo* invasion (24).

Local infusion of mAb428.2 in intracranial tumors (GBM09 cells) increased the number of tumor cells expressing the DNA damage marker phospho-H2A.X (Figure 6C–6D), matching the pro-apoptotic effect of this antibody in SC tumors. mAb428.2-treated tumors also showed decreased microvascular density, with significant reduction in the number of small vessels that are increased by fibulin-3 in GBM (28). The magnitude of this effect was comparable to a previously observed anti-angiogenic effect achieved by fibulin-3 knockdown in the same tumor model (28). Finally, mAb428.2 increased the infiltration of macrophages surrounding the tumor mass (Suppl. Figure S7B), suggesting an inflammatory effect similar to the one observed in SC tumors. Taken together, the results suggest that the anti-tumor effects of mAb428.2 in intracranial GBMs match a generalized inhibition of fibulin-3 mechanisms, together with increased anti-tumor inflammation.

Discussion

Most anti-tumor strategies with a focus on tumor ECM have concentrated on ECM-associated proteins rather than the structural components of the ECM. Successful strategies that have been translated to the clinical setting include inhibition of matrix-degrading metalloproteases (41, 42) and integrins (reviewed in (43)). In contrast, direct targeting of ECM molecules in GBM, such as hyaluronic acid, proteoglycans, and glycoproteins, has rarely advanced beyond experimental models. A notable exception is the monoclonal

antibody 81C6 that binds the ECM protein tenascin-C enriched in GBMs (44, 45). ^{131}I-labeled 81C6 (Neuradiab) was successfully tested for local radiotherapy of intracranial gliomas (46) and completed a phase II clinical trial (NCT00003478) before being discontinued in phase III (NCT00615186) for reasons unrelated to its efficacy. However, neither this antibody nor other approaches against ECM molecules have focused on identifying and blocking the signaling mechanisms that are triggered or regulated by these molecules in GBM.

In the present study we have identified a key motif exposed by the ECM protein fibulin-3 and demonstrated that this epitope is critical for the signaling functions of this protein in GBM. Moreover, we have developed and validated an antibody against this epitope and shown that it blocks the signaling functions of fibulin-3 *in vitro* and its tumor-promoting mechanisms *in vivo*. To our knowledge this is the first function-blocking antibody developed to inhibit pro-tumoral signaling mechanisms triggered by an ECM protein.

mAb428.2 showed significant efficacy against SC tumor xenografts, reducing tumor cell proliferation and increasing apoptosis. Moreover, the antibody promoted macrophage infiltration in the tumor, together with increased expression of inflammatory cytokines and decreased expression of M2/"tumor-promoting" macrophage markers in the tumor parenchyma (39). The reasons for the remarkable differences in the infiltrated macrophages of control- and mAb428.2-treated tumors are currently unknown because the effects of fibulin-3 on tumor-associated macrophages have not been studied. We can only speculate about the possibility that mAb428.2 disrupted an immunomodulatory effect of fibulin-3 on these immune cells. Alternatively, accumulation of mAb428.2 in the tumor could have been sufficient to initiate an inflammatory reaction that contributed to the observed anti-tumor effects. The increased necrosis in the core of mAb428.2-treated tumors (Suppl. Figure S5D) suggests that this anti-tumor reaction was highly efficient and tumor progression likely continued only after the treatment was discontinued.

mAb428.2 also showed efficacy against intracranial GBMs, increasing tumor cell apoptosis and decreasing vascularization. In addition, the antibody reduced GBM invasion in organotypic cultures of brain tissue, suggesting that it probably has a similar (not assessed) effect *in vivo*. Fibulin-3 is known to increase the invasion, apoptotic resistance, and vascularization of intracranial GBMs via Notch and ADAM17/NF-κB activation (25, 26, 28), therefore the effects of mAb428.2 match what would be expected from a widespread inhibition of fibulin-3 signaling in the tumor. We hypothesize that mAb428.2 prevents fibulin-3 from promoting tumor escape and progression mechanisms (e.g., dispersion and vascularization). Combined with anti-tumor innate immunity, these effects result in tumor cell death and extended survival.

The effects of our antibody may have been restricted in part by its rapid clearance and the requirement of repeated injections to "build up" in the tumors. This may have prevented IV-delivered mAb428.2 from reaching sufficient intracranial concentration to elicit anti-tumor effects. Another limitation was the limited solubility of mAb428.2 in phosphate- or lactate-buffered solutions, which could have also contributed to limited intratumoral accumulation. Nevertheless, our results suggest that mAb428.2 has significant anti-tumor effects that last

for as long as the antibody is delivered and able to accumulate in the tumor mass. These encouraging results warrant further optimization of mAb428.2 to continue improving these effects. Because the hybridoma mAb428.2 has been cloned and sequenced (sequences deposited in USPTO application #15/124,826; 2016), future work could proceed directly with recombinant variants of the antibody.

This study illustrates the feasibility of rationally developing biological agents to target the tumor ECM, which has been previously perceived as a passive barrier for drug efficacy (47) rather than a source of “druggable” targets (48). Targeting the ECM of malignant gliomas provides unique advantages such as the excellent accessibility of the targets; the ability to inhibit outside-in signaling mechanisms required for tumor progression; and the restricted expression of some ECM proteins to the tumor parenchyma (7, 49). Anti-ECM strategies could take advantage of a sizable group of novel targets that have been largely overlooked in GBMs and other solid tumors. We propose anti-fibulin-3 targeting as a strategy to disrupt signaling mechanisms in GBM and increase the efficacy of combination therapies for these malignant tumors.

Supplementary Material

Refer to Web version on PubMed Central for supplementary material.

Acknowledgments

Financial Support: This work was supported by grants from the National Institutes of Health (R01CA152065 and R21NS091436) and the B*Cured Foundation to MSV.

Bibliography

1. Howlader, NNA., Krapcho, M., Garshell, J., Miller, D., Altekruse, SF., Kosary, CL., Yu, M., Ruhl, J., Tatalovich, Z., Mariotto, A., Lewis, DR., Chen, HS., Feuer, EJ., Cronin, KA. SEER Cancer Statistics Review, 1975–2011. National Cancer Institute; Bethesda, MD: 2014. (http://seer.cancer.gov/csr/1975_2011/)
2. Fine HA. New strategies in glioblastoma: exploiting the new biology. Clin Cancer Res. 2015; 21:1984–1988. [PubMed: 25670220]
3. Friedmann-Morvinski D. Glioblastoma heterogeneity and cancer cell plasticity. Crit Rev Oncog. 2014; 19:327–336. [PubMed: 25404148]
4. Doucette T, Rao G, Rao A, Shen L, Aldape K, Wei J, et al. Immune heterogeneity of glioblastoma subtypes: extrapolation from the cancer genome atlas. Cancer Immunology Res. 2013; 1:112–122. [PubMed: 24409449]
5. Sengupta S, Mao G, Gokaslan ZS, Sampath P. Chimeric antigen receptors for treatment of glioblastoma: a practical review of challenges and ways to overcome them. Cancer Gene Ther. 2017; 24:121–129. [PubMed: 27767090]
6. Bellail AC, Hunter SB, Brat DJ, Tan C, Van Meir EG. Microregional extracellular matrix heterogeneity in brain modulates glioma cell invasion. Int J Biochem Cell Biol. 2004; 36:1046–1069. [PubMed: 15094120]
7. Viapiano, MS., Lawler, SE. Glioma invasion: Mechanisms and Therapeutic Challenges. In: Van Meir, E., editor. CNS Cancer: Models, Prognostic Factors and Targets. New Jersey: Humana Press; 2009. p. 1219-1252.
8. Viapiano MS, Matthews RT. From barriers to bridges: chondroitin sulfate proteoglycans in neuropathology. Trends Mol Med. 2006; 12:488–496. [PubMed: 16962376]

9. Wade A, Robinson AE, Engler JR, Petritsch C, James CD, Phillips JJ. Proteoglycans and their roles in brain cancer. The FEBS Journal. 2013; 280:2399–2417. [PubMed: 23281850]
10. Gritsenko PG, Ilina O, Friedl P. Interstitial guidance of cancer invasion. J Pathol. 2012; 226:185–199. [PubMed: 22006671]
11. Gladson CL. The extracellular matrix of gliomas: modulation of cell function. J Neuropathol Exp Neurol. 1999; 58:1029–1040. [PubMed: 10515226]
12. Brosicke N, Faissner A. Role of tenascins in the ECM of gliomas. Cell Adhesion & Migration. 2015; 9:131–140. [PubMed: 25695402]
13. Balvers RK, Kleijn A, Kloezeman JJ, French PJ, Kremer A, van den Bent MJ, et al. Serum-free culture success of glial tumors is related to specific molecular profiles and expression of extracellular matrix-associated gene modules. Neuro-Oncol. 2013; 15:1684–1695. [PubMed: 24046260]
14. Patel AP, Tirosh I, Trombetta JJ, Shalek AK, Gillespie SM, Wakimoto H, et al. Single-cell RNA-seq highlights intratumoral heterogeneity in primary glioblastoma. Science. 2014; 344:1396–1401. [PubMed: 24925914]
15. Brennan CW, Verhaak RG, McKenna A, Campos B, Noushmehr H, Salama SR, et al. The somatic genomic landscape of glioblastoma. Cell. 2013; 155:462–477. [PubMed: 24120142]
16. Martinez-Quintanilla J, He D, Wakimoto H, Alemany R, Shah K. Encapsulated stem cells loaded with hyaluronidase-expressing oncolytic virus for brain tumor therapy. Mol Ther. 2015; 23:108–118. [PubMed: 25352242]
17. Jaime-Ramirez AC, Dmitrieva N, Yoo JY, Banasavadi-Siddegowda Y, Zhang J, Relation T, et al. Humanized chondroitinase ABC sensitizes glioblastoma cells to temozolomide. J Gene Med. 2017; 19(3)doi: 10.1002/jgm.2942
18. Ulbricht U, Eckerich C, Fillbrandt R, Westphal M, Lamszus K. RNA interference targeting protein tyrosine phosphatase zeta/receptor-type protein tyrosine phosphatase beta suppresses glioblastoma growth in vitro and in vivo. J Neurochem. 2006; 98:1497–1506. [PubMed: 16923162]
19. Dwyer CA, Bi WL, Viapiano MS, Matthews RT. Brevican knockdown reduces late-stage glioma tumor aggressiveness. J Neurooncol. 2014; 120:63–72. [PubMed: 25052349]
20. Akabani G, Cokgor I, Coleman RE, Gonzalez Trotter D, Wong TZ, Friedman HS, et al. Dosimetry and dose-response relationships in newly diagnosed patients with malignant gliomas treated with iodine-131-labeled anti-tenascin monoclonal antibody 81C6 therapy. Int J Radiat Oncol Biol Phys. 2000; 46:947–958. [PubMed: 10705017]
21. Akabani G, Reardon DA, Coleman RE, Wong TZ, Metzler SD, Bowsher JE, et al. Dosimetry and radiographic analysis of 131I-labeled anti-tenascin 81C6 murine monoclonal antibody in newly diagnosed patients with malignant gliomas: a phase II study. J Nucl Med. 2005; 46:1042–1051. [PubMed: 15937318]
22. Kobayashi N, Kostka G, Garbe JH, Keene DR, Bachinger HP, Hanisch FG, et al. A comparative analysis of the fibulin protein family. Biochemical characterization, binding interactions, and tissue localization. J Biol Chem. 2007; 282:11805–11816. [PubMed: 17324935]
23. Giltay R, Timpl R, Kostka G. Sequence, recombinant expression and tissue localization of two novel extracellular matrix proteins, fibulin-3 and fibulin-4. Matrix Biol. 1999; 18:469–480. [PubMed: 10601734]
24. Hu B, Thirtamara-Rajamani KK, Sim H, Viapiano MS. Fibulin-3 Is Uniquely Upregulated in Malignant Gliomas and Promotes Tumor Cell Motility and Invasion. Mol Cancer Res. 2009; 7:1756–1770. [PubMed: 19887559]
25. Hu B, Nandhu MS, Sim H, Agudelo-Garcia PA, Saldivar JC, Dolan CE, et al. Fibulin-3 promotes glioma growth and resistance through a novel paracrine regulation of Notch signaling. Cancer Res. 2012; 72:3873–3785. [PubMed: 22665268]
26. Nandhu MS, Kwiatkowska A, Bhaskaran V, Hayes J, Hu B, Viapiano MS. Tumor-derived fibulin-3 activates pro-invasive NF-kappaB signaling in glioblastoma cells and their microenvironment. Oncogene. 2017; 36:4875–4886. [PubMed: 28414309]
27. Hiddingh L, Tannous BA, Teng J, Tops B, Jeuken J, Hulleman E, et al. EFEMP1 induces gamma-secretase/Notch-mediated temozolomide resistance in glioblastoma. Oncotarget. 2014; 5:363–374. [PubMed: 24495907]

28. Nandhu MS, Hu B, Cole SE, Erdreich-Epstein A, Rodriguez-Gil DJ, Viapiano MS. Novel paracrine modulation of Notch-DLL4 signaling by fibulin-3 promotes angiogenesis in high-grade gliomas. Cancer Res. 2014; 74:5435–5448. [PubMed: 25139440]
29. Song EL, Hou YP, Yu SP, Chen SG, Huang JT, Luo T, et al. EFEMP1 expression promotes angiogenesis and accelerates the growth of cervical cancer in vivo. Gynecol Oncol. 2011; 121:174–180. [PubMed: 21163514]
30. Pass HI, Levin SM, Harbut MR, Melamed J, Chiriboga L, Donington J, et al. Fibulin-3 as a blood and effusion biomarker for pleural mesothelioma. N Engl J Med. 2012; 367:1417–1427. [PubMed: 23050525]
31. Chen J, Wei D, Zhao Y, Liu X, Zhang J. Overexpression of EFEMP1 correlates with tumor progression and poor prognosis in human ovarian carcinoma. PLoS One. 2013; 8:e78783. [PubMed: 24236050]
32. Fenn AM, Hall JC, Gensel JC, Popovich PG, Godbout JP. IL-4 signaling drives a unique arginase+/IL-1beta+ microglia phenotype and recruits macrophages to the inflammatory CNS: consequences of age-related deficits in IL-4Ralpha after traumatic spinal cord injury. J Neurosci. 2014; 34:8904–8917. [PubMed: 24966389]
33. Nagelkerke A, Span PN. Staining Against Phospho-H2AX (gamma-H2AX) as a Marker for DNA Damage and Genomic Instability in Cancer Tissues and Cells. Adv Exp Med Biol. 2016; 899:1–10. [PubMed: 27325258]
34. Kilkenny C, Browne W, Cuthill IC, Emerson M, Altman DG. Group NCRRGW. Animal research: reporting in vivo experiments: the ARRIVE guidelines. Br J Pharmacol. 2010; 160:1577–1579. [PubMed: 20649561]
35. Wang Z, Cao CJ, Huang LL, Ke ZF, Luo CJ, Lin ZW, et al. EFEMP1 promotes the migration and invasion of osteosarcoma via MMP-2 with induction by AEG-1 via NF-kappaB signaling pathway. Oncotarget. 2015; 6:14191–14208. [PubMed: 25987128]
36. Kelley LA, Mezulis S, Yates CM, Wass MN, Sternberg MJE. The Phyre2 web portal for protein modeling, prediction and analysis. Nat Protocols. 2015; 10:845–858. [PubMed: 25950237]
37. Marmorstein LY, Munier FL, Arsenijevic Y, Schorderet DF, McLaughlin PJ, Chung D, et al. Aberrant accumulation of EFEMP1 underlies drusen formation in Malattia Leventinese and age-related macular degeneration. Proc Natl Acad Sci USA. 2002; 99:13067–13072. [PubMed: 12242346]
38. Freireich EJ, Gehan EA, Rall DP, Schmidt LH, Skipper HE. Quantitative comparison of toxicity of anticancer agents in mouse, rat, hamster, dog, monkey, and man. Cancer Chemother Rep. 1966; 50:219–244. [PubMed: 4957125]
39. Shi Y, Ping YF, Zhou W, He ZC, Chen C, Bian BS, et al. Tumour-associated macrophages secrete pleiotrophin to promote PTPRZ1 signalling in glioblastoma stem cells for tumour growth. Nature Communications. 2017; 8:15080.doi: 10.1038/ncomms15080
40. Reinhold WC, Sunshine M, Liu H, Varma S, Kohn KW, Morris J, et al. CellMiner: a web-based suite of genomic and pharmacologic tools to explore transcript and drug patterns in the NCI-60 cell line set. Cancer Res. 2012; 72:3499–3511. [PubMed: 22802077]
41. Levin VA, Phuphanich S, Yung WK, Forsyth PA, Maestro RD, Perry JR, et al. Randomized, double-blind, placebo-controlled trial of marimastat in glioblastoma multiforme patients following surgery and irradiation. J Neurooncol. 2006; 78:295–302. [PubMed: 16636750]
42. Groves MD, Puduvalli VK, Conrad CA, Gilbert MR, Yung WK, Jaeckle K, et al. Phase II trial of temozolomide plus marimastat for recurrent anaplastic gliomas: a relationship among efficacy, joint toxicity and anticonvulsant status. J Neurooncol. 2006; 80:83–90. [PubMed: 16639492]
43. Paolillo M, Serra M, Schinelli S. Integrins in glioblastoma: Still an attractive target? Pharmacol Res. 2016; 113:55–61. [PubMed: 27498157]
44. Bourdon MA, Coleman RE, Blasberg RG, Groothuis DR, Bigner DD. Monoclonal antibody localization in subcutaneous and intracranial human glioma xenografts: paired-label and imaging analysis. Anticancer Res. 1984; 4:133–140. [PubMed: 6465851]
45. Lee Y, Bullard DE, Humphrey PA, Colapinto EV, Friedman HS, Zalutsky MR, et al. Treatment of intracranial human glioma xenografts with 131I-labeled anti-tenascin monoclonal antibody 81C6. Cancer Res. 1988; 48:2904–2910. [PubMed: 2452014]

46. Reardon DA, Zalutsky MR, Bigner DD. Antitenascin-C monoclonal antibody radioimmunotherapy for malignant glioma patients. Expert Rev Anticancer Ther. 2007; 7:675–687. [PubMed: 17492931]

47. Huxley-Jones J, Foord SM, Barnes MR. Drug discovery in the extracellular matrix. Drug Discovery Today. 2008; 13:685–94. [PubMed: 18583179]

48. Jarvelainen H, Sainio A, Koulu M, Wight TN, Penttinen R. Extracellular matrix molecules: potential targets in pharmacotherapy. Pharmacol Rev. 2009; 61:198–223. [PubMed: 19549927]

49. Shimizu T, Kurozumi K, Ishida J, Ichikawa T, Date I. Adhesion molecules and the extracellular matrix as drug targets for glioma. Brain Tumor Pathol. 2016; 33:97–106. [PubMed: 26992378]

Translational Relevance

The molecular heterogeneity and invasive ability of glioblastoma (GBM) cells are two major obstacles for successful therapy of these malignant brain cancers. Targeting the tumor extracellular matrix (ECM) may help overcome these obstacles because ECM molecules secreted by tumor cells are necessary for invasion and relatively conserved across the tumor parenchyma. New strategies against the ECM must first identify functional domains in ECM targets and develop reagents to block those domains and disrupt signaling initiated and regulated by ECM molecules. We have developed a function-blocking antibody against a GBM-enriched ECM protein (fibulin-3) that is a “first in class” reagent able to inhibit pro-tumoral signaling and reduce GBM progression. Anti-ECM reagents may exploit a niche that is currently under-explored, leading towards more efficient combination treatments for GBM and potentially other solid tumors.

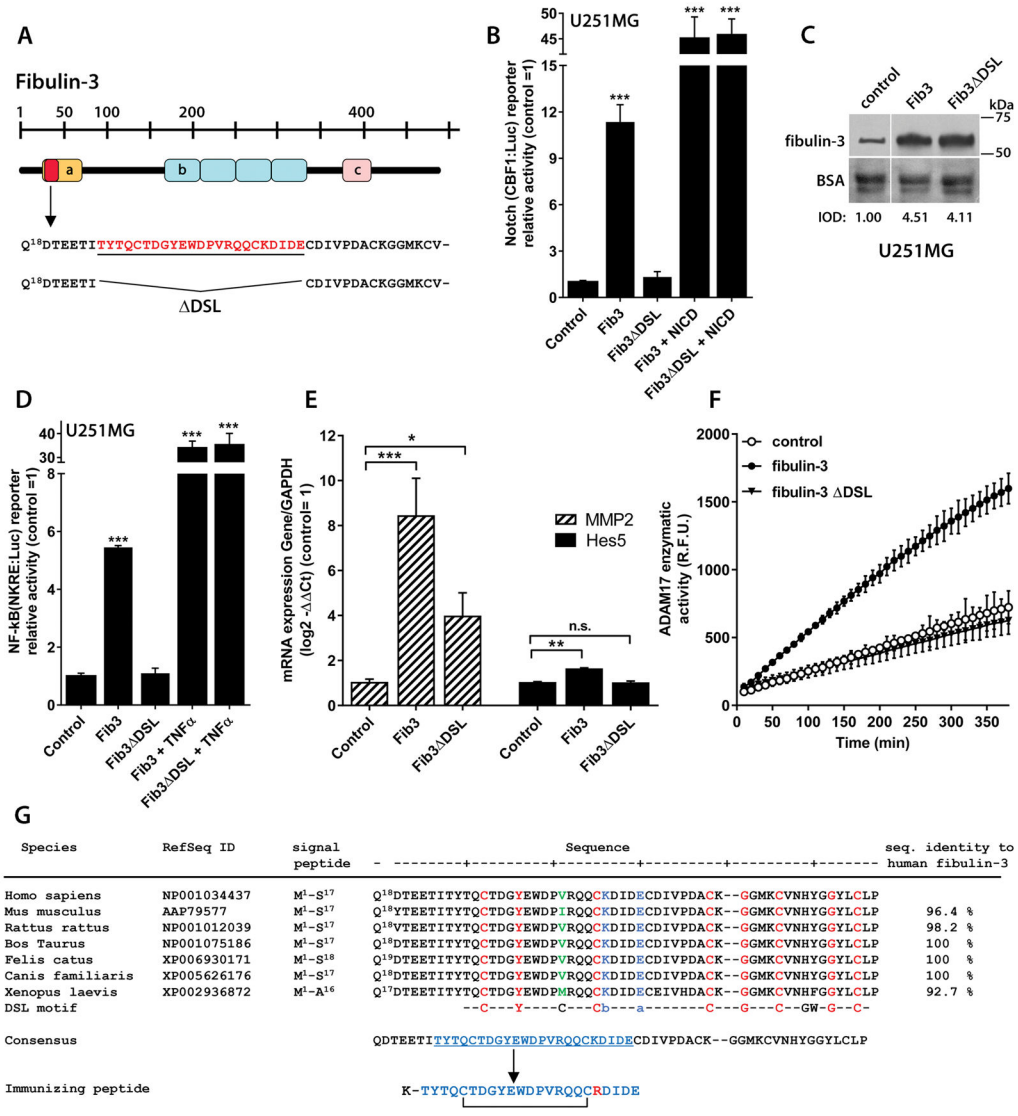

Figure 1. Fibulin-3 signaling depends on a critical N-terminal sequence

A) Representation of fibulin-3 structure and N-terminal localization of the DSL-like epitope (Thr^{25}-Glu^{47}, underlined) deleted in fibulin-3ΔDSL (*a:* Ca^{++}-binding EGF-like domain; *b:* EGF-like repeats; *c:* fibulin consensus domain). **B)** The activity of a Notch-dependent luciferase reporter in U251MG cells was increased by fibulin-3 transiently transfected for 24h but not by fibulin-3ΔDSL (control: empty expression vector). None of the fibulin-3 constructs affected Notch reporter activity driven by a constitutive control (NICD). **C**) Internal transfection controls (10 μg total protein/lane) show that fibulin-3 and fibulin-3ΔDSL were expressed at similar levels in the conditioned medium of U251MG cells; total BSA in the medium was used as loading control (IOD: integrated optical density, relative to the control transfection). **D**) Transfected fibulin-3, but not fibulin-3ΔDSL, also increased the activity of a NF-κB-dependent reporter in U251MG cells (same experimental design as in (**B**)). For a positive control of NF-κB-driven reporter activity the cells were treated with TNFα (10 ng/ml, 6h). **E**) U251MG cells transfected with fibulin-3 cDNA and

processed after 24h showed increased mRNA expression of Notch-regulated genes (*MMP2* and *HES5*); transfection of fibulin-3ΔDSL had a much smaller or absent effect. Analyses in (**B**)–(**E**) by 1-way ANOVA: *** p< 0.001; ** p<0.01; * p<0.05 for each reporter or gene. **F)** Overexpression of fibulin-3 in U251MG cells significantly increased the proteolytic activity of ADAM17 in cell lysates (*R.F.U.*: relative fluorescence units); in contrast, transfection of fibulin-3ΔDSL was undistinguishable from control cells (all cells processed 24h post-transfection). **G)** Alignment of the N-terminal sequence of fibulin-3 against the canonical DSL-motif of Notch ligands; this sequence is very well conserved across species. Amino acids in red indicate conservation of DSL between fibulin-3 and Notch ligands and those in green show a major divergence from the consensus DSL motif (*b*: basic amino acid; *a*: acidic amino acid). The peptide chosen for immunization corresponds to Thr^{25}-Glu^{47} of human fibulin-3 but has Lys^{43} replaced with Arg as indicated in the Methods section.

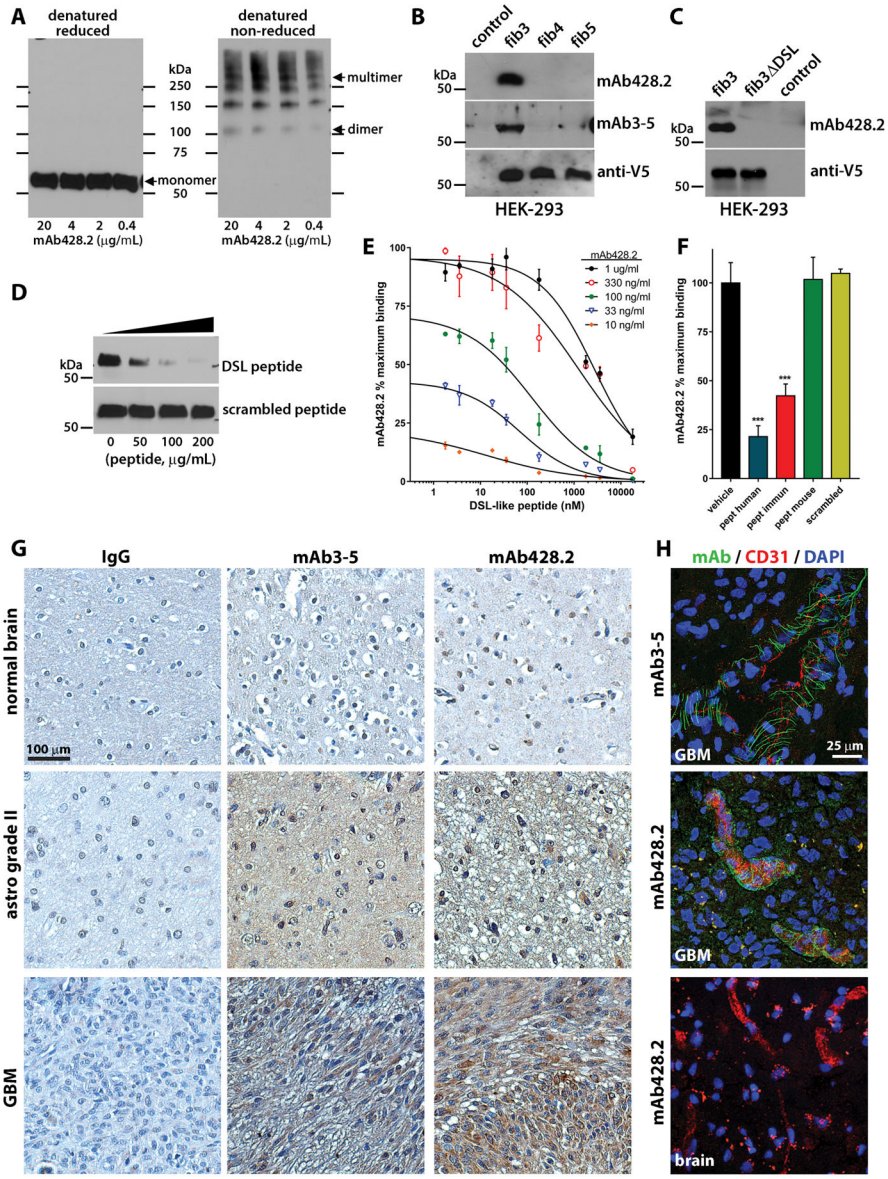

Figure 2. Characterization of anti-fibulin-3 mAb428.2

A) Western blots showing detection of purified fibulin-3 by mAb428.2 in reduced and non-reduced conditions (200 ng protein/lane). The arrows indicate the position of the 55-kDa monomer, 110-kDa dimer, and high-Mw multimer (fibrillar) forms of fibulin-3. **B)** Western blots of serum-free conditioned medium from HEK293 cells (10 μg total protein/lane) expressing V5-tagged fibulins -3, -4, or -5. Blots were probed with an antibody against the V5 epitope or with the anti-fibulin-3 antibodies mAb428.2 and mAb3-5. The control lane contains medium from untransfected cells. **C)** Western blots of serum-free conditioned medium from HEK293 cells expressing V5-tagged full-length fibulin-3 (*fib3*) and fibulin-3ΔDSL that lacks the target epitope of mAb428.2. **D)** Detection of purified fibulin-3 (200 ng/lane) by mAb428.2 was inhibited by the DSL-like peptide from fibulin-3 (Thr^{25}-Glu^{47}) but not by a scrambled version of this peptide. **E)** Microtiter plates were coated with

BSA-conjugated DSL-like peptide (1,000 ng/ml) and different concentrations of mAb428.2 were used to detect the epitope by indirect-ELISA. mAb428.2 binding to BSA-conjugated peptide was displaced by incubation with free DSL-like peptide following a simple competitive model (analyzed in Suppl. Figure S2A). **F)** Microtiter plates were coated with purified fibulin-3 (200 ng/ml) and mAb428.2 (1 μg/ml) was used to detect the protein by indirect-ELISA. Binding of the antibody was inhibited by the DSL-like peptide from human fibulin-3 (*pept human*) and the modified peptide used for immunization (*pept immun*); *** $p<0.001$, 1-way ANOVA. However, the DSL-like peptide from mouse fibulin-3 (*pept mouse*, containing Ile^{38} instead of Val^{38}) was unable to displace mAb428.2 binding. All peptides were tested at a maximum concentration of 50 μg/ml (18 μM). **G)** Immunohistochemistry of paraffin-processed tissue sections using mAb428.2 or mAb3-5 showed similar detection of fibulin-3, which increased with tumor grade. The sparse nuclear staining observed with both antibodies is non-specific. Control staining was performed with non-immune mouse IgG. **H)** Immunohistochemistry of frozen GBM sections using mAb428.2 or mAb3-5 showed a characteristic perivascular fibrillar pattern previously described (28). mAb428.2 did not detect perivascular fibulin-3 in blood vessels from normal brain adjacent to the tumor (*brain*), as expected. Vessels were stained with an antibody against endothelial CD31.

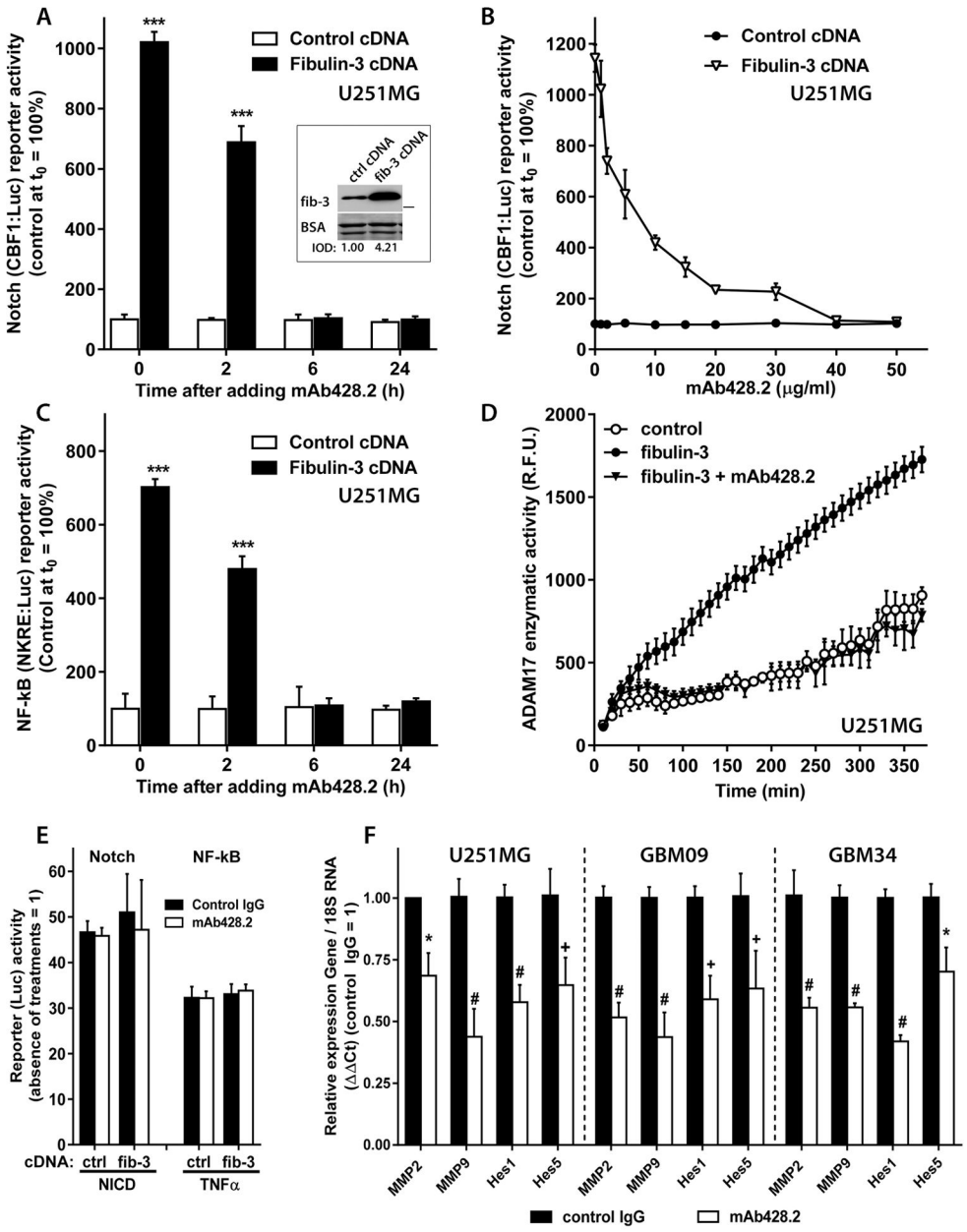

Figure 3. mAb428.2 inhibits fibulin-3 signaling in glioblastoma cells

A) U251MG stably expressing a Notch-dependent reporter (*CBF1:Luc*) were transfected with fibulin-3 or control cDNAs and after 24h treated with 50 μg/ml of mAb428.2. The antibody inhibited the enhancing effect of fibulin-3 on Notch activity within 6h. The inset shows the level of fibulin-3 overexpression in the cells, quantified as shown in Figure **1C. B)** Same experimental design as in **(A)** but mAb428.2 was added at different concentrations for 6h. Fibulin-3-enhanced Notch activity was completely blocked by mAb428.2 at concentrations above 30 μg/ml. **C)** Same experimental design as in **(A)**, using cells stably expressing a NF-κB-dependent reporter (*NKRE:Luc*). mAb428.2 inhibited the enhancing effect of fibulin-3 on NF-κB activity within 6h. Firefly Luciferase activity of the reporters

was normalized to a transfected *Renilla* Luciferase control as indicated in the Methods. Significant differences in (**A**) and (**C**): *** $p<0.001$ (2-way ANOVA). **D)** U251MG cells were transfected with fibulin-3 or control cDNAs and lysed after 24h; the lysates were incubated with an ADAM17 fluorogenic substrate to measure enzymatic activity in presence or absence of mAb428.2. Fibulin-3 overexpression increased ADAM17 activity but this effect was completely abolished when mAb428.2 (50 μg/ml) was present in the reaction mixture. Treatment of cells or lysates with non-immune IgG in experiments (**A–D**) had no effects on reporters or enzymatic activity. **E)** U251MG cells transfected with NICD cDNA (for 24h) to activate the Notch reporter, or treated with TNFα (10 ng/ml, 6h) to activate the NF-κB reporter, showed no changes in reporter activity when they were co-transfected with fibulin-3 cDNA or incubated with antibodies (50 μg/ml). **F**) U251MG cells and two GSC cultures (GBM09 and GBM34) were treated with mAb428.2 (50 μg/ml) or a control IgG for 24h and then processed to measure mRNA expression of Notch- and NF-κB-dependent genes. mAb428.2 reduced the expression of the four tested genes compared to control IgG treatment (* $p<0.05$; + $p<0.01$; # $p< 0.001$, by 2-way ANOVA for each cell type).

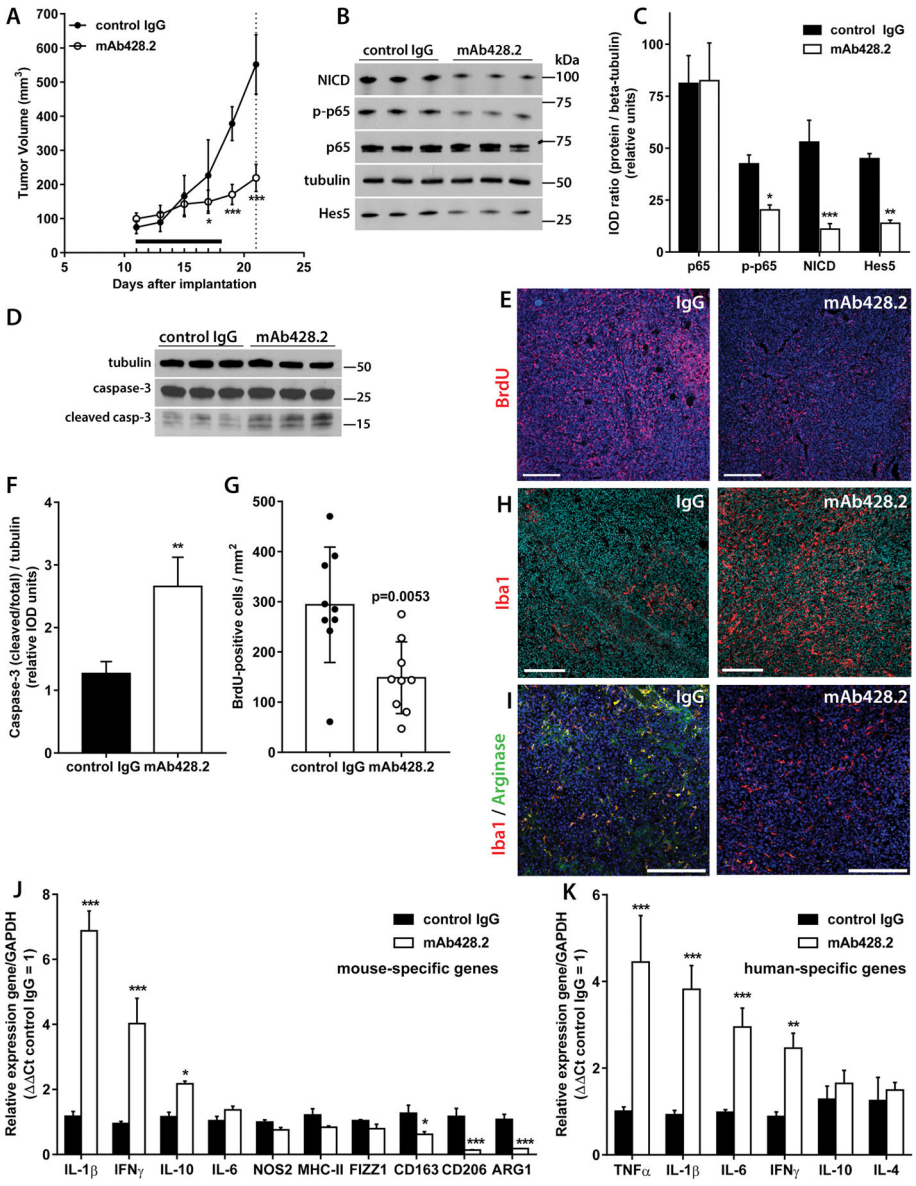

Figure 4. mAb428.2 inhibits tumor growth and increases inflammatory macrophage infiltration in the tumor

A) Mice carrying bilateral SC GBM34 tumors (N=5/group) were treated with daily injections of mAb428.2 or control IgG for eight days (8 x 30 mg/kg IV, horizontal bar). Tumor growth was significantly inhibited in mAb428.2-treated mice (* $p< 0.05$; *** $p<0.001$; repeated measures ANOVA). Animals were euthanized three days after the last injection (dashed line) and their tumors were processed for the rest of the experiments in the figure **B–C)** Expression of Notch1 Intracellular Domain (*NICD*) and the transcription factors Hes5 and RelA/p65 (and phospho-p65) was probed by Western blot and quantified by densitometry (*IOD:* integrated optical density). mAb428.2 treatment significantly reduced expression of NICD, Hes5, and phospho-p65, suggesting inhibition of fibulin-3 effects on Notch and NF-κB signaling (* $p<0.05$; ** $p<0.01$; *** $p<0.001$; Student's t-test for each marker). **D)** Expression of full-length and cleaved caspase-3 (*casp-3*) was probed in

three representative tumors per treatment. **E**) Uptake of BrdU was detected by immunohistochemistry in five tumors per treatment; the images show representative staining results. **F**) Quantitative analysis of caspase-3 expression from (**D**) shows increased caspase cleavage in mAb428.2-treated tumors (** $p<0.01$; Student's t-test). **G**) Quantitative analysis of BrdU staining from (**E**); each dot represents a tissue section. mAb428.2 significantly reduced BrdU uptake (analysis by Mann-Whitney U test). **H)** Increased macrophage infiltration in mAb428.2-treated tumors, detected by Iba1-positive staining. **I**) Comparison of tissue sections with similar number of macrophages in both treatments revealed co-expression of Arginase-1 with Iba1-positive cells in control-treated tumors but very low or absent Arginase-1 in macrophages of mAb428.2-treated tumors. **J**) Tumor treatment with mAb428.2 correlated with increased mRNA expression of the host's inflammatory cytokines and decreased expression of M2-macrophage markers (*CD163*, *CD206*, and *ARG1*); all genes were detected by qRT-PCR with mouse-specific primers. **K**) Tumor treatment with mAb428.2 also correlated with increased mRNA expression of inflammatory cytokines in the tumor cells, detected by qRT-PCR with human-specific primers. Results in (**J**) and (**K**) were analyzed by Student's t-test corrected for multiple comparisons (* $p<0.05$; ** $p<0.01$; *** $p<0.001$). Bars in all the histological images: 200 μm.

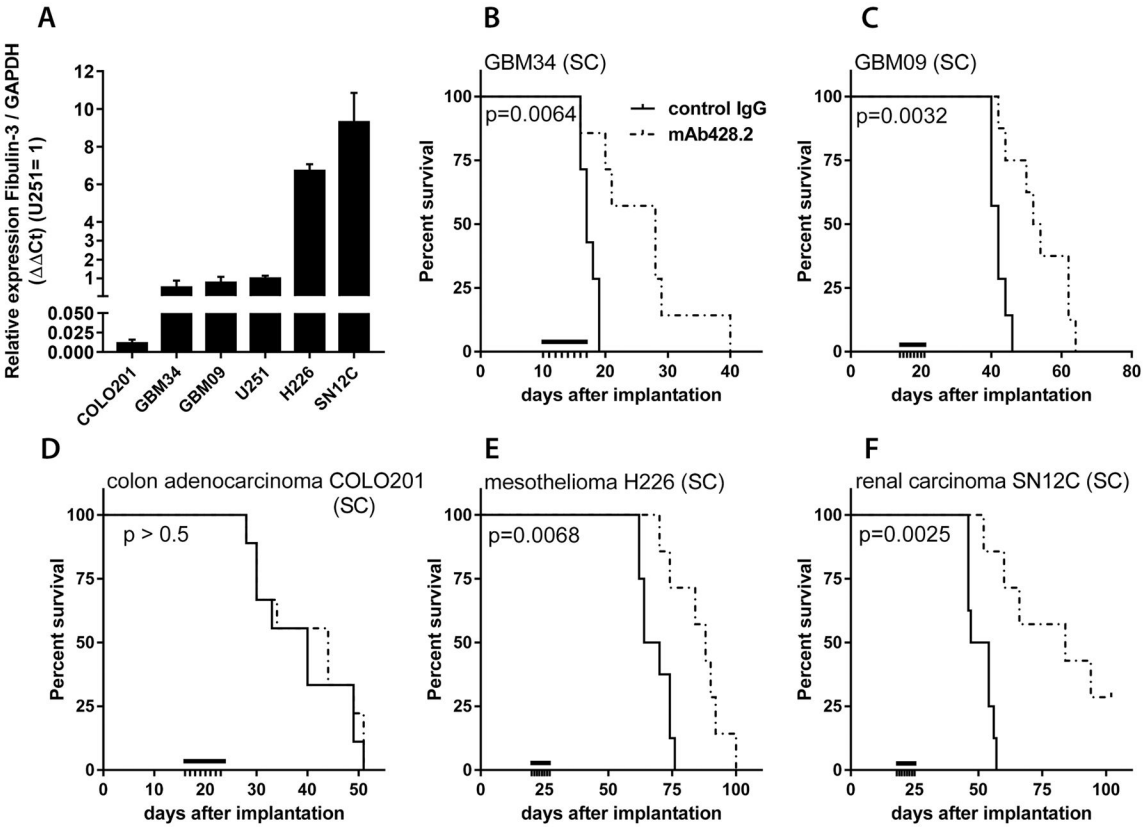

Figure 5. mAb428.2 extends survival of mice carrying fibulin-3-secreting tumors

A) Comparative expression of fibulin-3 mRNA in a conventional GBM cell line (U251MG), GSC cultures (GBM34 and GBM09), and three cell lines from the NCI-60 collection (COLO201 colon carcinoma; H226 mesothelioma; and SN12C renal cell carcinoma). **B–F**) Mice carrying SC tumors derived from the cells compared in (**A**) were treated with mAb428.2 (8 x 30 mg/kg q24h IV) or non-immune control IgG when the tumors reached a threshold volume of 100 mm^3 (black bars indicate the treatment period, N=8/group). mAb428.2 extended the median survival of mice carrying fibulin-3-expressing tumors (analysis by log-rank test for each tumor model) but failed to improve the survival of mice carrying COLO201 tumors that have negligible fibulin-3 expression.

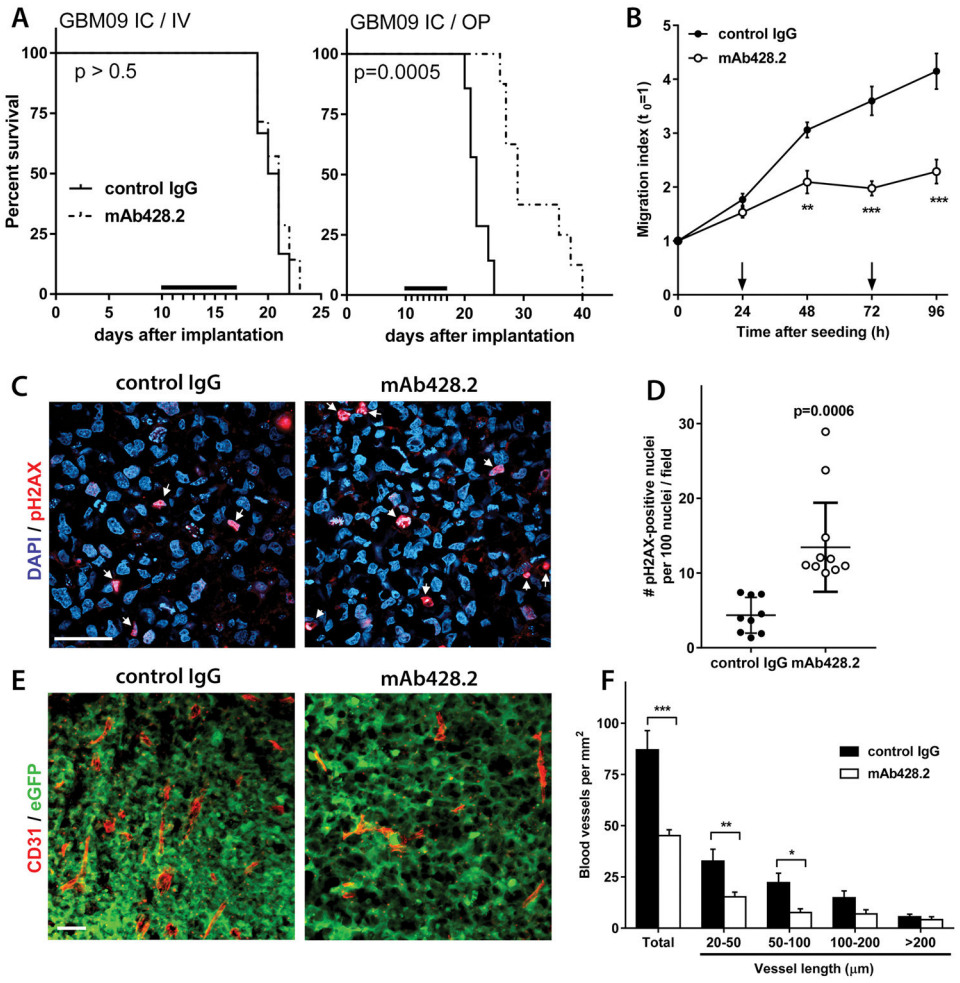

Figure 6. mAb428.2 has anti-tumor effects in intracranial GBMs

A) Mice carrying intracranial (*IC*) xenografts of GBM09 cells were treated with mAb428.2 injected IV as in Figure 5, or locally infused with an osmotic pump (*OP*) as indicated in the Methods (black bars indicate the treatment period, N=8/group). Only animals that received local mAb428.2 infusion showed improved survival (curves analyzed by log-rank test). **B**) Tumor spheres of GBM09 cells were seeded on cultured brain slices and their invasion through brain tissue was monitored by microscopy as described in the Methods (24). Addition of mAb428.2 to the culture medium (200 μg/ml, arrows) significantly inhibited cell invasion (** p< 0.01; *** p<0.001; 2-way ANOVA for repeated measures). **C–D**) Tissue sections from intracranial tumors (GBM09) treated with locally-delivered antibody were processed for immunohistochemistry to detect phospho-Histone H2A.X (*pH2AX*, N=5/group). Quantitative analysis showed a significant increase of pH2AX-positive nuclei in mAb428.2-treated tumors (Mann-Whitney U test). **E–F**) Intracranial tumors (GBM09-eGFP) were also processed to detect and quantify blood vessels as described (28) (CD31 staining, N=5/group). mAb428.2-treated tumors had a significant reduction of microvascular density, caused by a lower number of small vessels (* p<0.05; ** p< 0.01; *** p<0.001; 2-way ANOVA). Bars in all the histological images: 50 μm